Bioprocess Biosyst Eng (2015) 38:251–261
DOI 10.1007/s00449-014-1264-8

ORIGINAL PAPER

High cell density culture with *S. cerevisiae* CEN.PK113-5D for IL-1β production: optimization, modeling, and physiological aspects

Carmine Landi · Lucia Paciello · Elisabetta de Alteriis · Luca Brambilla · Palma Parascandola

Received: 24 April 2014 / Accepted: 29 July 2014 / Published online: 9 August 2014

Abstract *Saccharomyces cerevisiae* CEN.PK113-5D, a strain auxotrophic for uracil belonging to the CEN.PK family of the yeast *S. cerevisiae*, was cultured in aerated fed-batch reactor as such and once transformed to express human interleukin-1β (IL-1β), aiming at obtaining high cell densities and optimizing IL-1β production. Three different exponentially increasing glucose feeding profiles were tested, all of them "in theory" promoting respiratory metabolism to obtain high biomass/product yield. A non-structured non-segregated model was developed to describe the performance of *S. cerevisiae* CEN.PK113-5D during the fed-batch process and, in particular, its capability to metabolize simultaneously glucose and ethanol which derived from the precedent batch growth. Our study showed that the proliferative capacity of the yeast population declined along the fed-batch run, as shown by the exponentially decreasing specific growth rates on glucose. Further, a shift towards fermentative metabolism occurred. This shift took place earlier the higher was the feed rate and was more pronounced in the case of the recombinant strain. Determination of some physiological markers (acetate production, intracellular ROS accumulation, catalase activity and cell viability) showed that neither poor oxygenation nor oxidative stress was responsible for the decreased specific growth rate, nor for the shift to fermentative metabolism.

Keywords *S. cerevisiae* · High cell density cultures · Yeast growth modeling · Metabolic shift · Auxotrophic yeasts

Abbreviations

β	Inhibition factor of glucose on ethanol consumption
E	Ethanol concentration at time t (g L^{-1})
E_0	Ethanol concentration at the end of batch phase/ beginning of fed-batch phase (g L^{-1})
F	Glucose flow rate at time t (L h^{-1})
F_0	Glucose flow rate at the beginning of fed-batch phase (L h^{-1})
G	Residual glucose concentration at time t (g L^{-1})
G_0	Residual glucose concentration at the beginning of fed-batch phase (g L^{-1})
G_R	Glucose concentration in the feeding (g L^{-1})
k_d	Specific death rate (h^{-1})
$(k_S)_E$	Ethanol saturation constant (g L^{-1})
$(\mu_{max})_E$	Maximum specific growth rate on ethanol (h^{-1})
$(\mu_G)_i$	Specific growth rate on glucose in the i th interval (h^{-1})
t	Arbitrary time of fed-batch run (h^{-1})
t_{EC}	Time of fed-batch run when ethanol finished to be consumed and the variation of specific growth rate on glucose equation occurs (h)
t_{EP}	Time of fed-batch run when ethanol begins to be accumulated (h)
V	Broth culture volume (L)
X	Viable biomass concentration at time t (g cell d.w. L^{-1})

C. Landi · L. Paciello · P. Parascandola (✉)
Dep. Ingegneria Industriale, Università Di Salerno,
Via Giovanni Paolo II, 132 Fisciano, 84084 Salerno, Italy
e-mail: pparascandola@unisa.it

E. de Alteriis
Dep. Biologia, Università degli Studi di Napoli "Federico II",
Via Cinthia, 80100 Naples, Italy

L. Brambilla
Dep. Biotecnologie e Bioscienze, Università Milano-Bicocca,
Piazza Della Scienza, 20126 Milan, Italy

X_0	Initial viable biomass concentration (g cell d.w. L^{-1})
$(Y_{X/G})_i$	Biomass yield on glucose in the i-th interval of fed-batch run (g cell d.w. g glucose^{-1})
$(Y_{X/G})_1$	Biomass yield on glucose in the interval $0 \leq t < t_{EC}$ (g cell d.w. g glucose^{-1})
$(Y_{X/G})_2$	Biomass yield on glucose in the interval $t \geq t_{EC}$ (g cell d.w. g glucose^{-1})
$(Y_{X/E})_S$	Biomass yield on ethanol as substrate in the interval $0 \leq t < t_{EC}$ (g cell d.w. g ethanol^{-1})
$(Y_{E/X})_P$	Ethanol produced per unit of biomass in the interval $t \geq t_{EP}$ (g ethanol g cell d.w.$^{-1}$)

Introduction

The major objective of fermentation in both research and industry is to maximize product yield and volumetric productivity [1, 2], which is a function of cell density.

To obtain high cell density cultivation (HCDC), fed-batch culture has been proven a successful system due to the possibility of extending working time, controlling substrate supply to the reactor and, consequently, avoiding the effects of overflow metabolism and catabolite repression [2].

Fed-batch culture is the system mainly used to produce recombinant proteins with the glucose-sensitive yeast *Saccharomyces cerevisiae* [3, 4]. Glucose-sensitive yeasts display a respiratory metabolism with high biomass yield only when sugar supply is low and its concentration does not exceed a threshold value, above which overflow metabolism with ethanol production is triggered [5]. However, high cell densities, especially in the typical industrial conditions, may cause some strong constraints to an efficient mass distribution, while the expression of a heterologous product at high level can result in an overloading of cellular metabolism. Cell growth and biomass yield can be heavily influenced by the two phenomena above, resulting in poor process performances also using low sugar feedings.

With the aim to study and model the deviations induced by cultural conditions on process performance, in the present work, we have analyzed the growth of a yeast strain expressing a heterologous gene and growing to high cell density. As model organism we chose *S. cerevisiae* CEN.PK113-5D strain, since it was found to be the best performer among the auxotrophic components of the CEN.PK family [6]. In the present work, to discriminate the effects given by a heterologous metabolic burden over those related to the cultural conditions, we have compared the growth parameters of CEN.PK113-5D expressing an heterologous product against those of the non-transformed strain. The recombinant strain carries, on the episomal pIA1 derivative [7], the coding sequence for human interleukin-1β (IL-1β) gene fused with the regulatory sequences of *PIR4* gene [8] that promotes IL-1β secretion to the growth medium [9].

The first stage of a fed-batch cultivation carried out with *S. cerevisiae* cells is usually a standard batch process built up to develop the inoculum size for the fed-phase. Indeed, just before the initial substrate is exhausted, a concentrated sugar solution is fed to the fermenter at an exponentially increasing feed rate which allows the yeast population to grow at a constant specific growth rate so achieving a high volumetric productivity [10]. In the perspective to optimize the yeast performances of both, cell growth performances were studied by varying the feeding rate of the carbon source to the fermenter, taking care that oxygen was not limiting. During every fed-batch run, cell density and concentration profiles for residual glucose and ethanol were determined. In the case of the recombinant strain, IL-1β was also determined in the culture supernatants collected during the fed-batch runs. Three different specific glucose flow rates were chosen, far enough from the critical value of glucose feeding rate [11], to avoid overflow metabolism and consequent ethanol production. However, in all experimental conditions tested, we detected a progressive and unexpected diminution of biomass yield.

The experimental approach to the investigation was implemented by modeling the fed-batch reactor through a non-structured non-segregated model, to describe the performance of *S. cerevisiae* CEN.PK113-5D in a complex environment such as that arising during the fed-batch process. In particular, the model was developed aiming at describing the simultaneous capability of *S. cerevisiae* CEN.PK113-5D strain to metabolize glucose and ethanol and to point out the observed decrease in biomass yield.

Finally, some physiological markers were determined in the attempt to relate their appearance with the observed decrease of cellular yield.

Materials and Methods

Strain and Transformation

The *Saccharomyces cerevisiae* strain used in this work, CEN.PK113-5D (*Mata ura3-52 HIS3 LEU2 TRP1 MAL2-8c SUC2*), was provided by the Laboratory of Biotechnology, University of Milano-Bicocca (Italy).

Saccharomyces cerevisiae CEN.PK113-5D strain was transformed with the expression vector pIA1 derived from the multicopy plasmid YEplac 195 [7], containing *URA3* as selectable marker and the human interleukin-1β (*IL-1β*) gene functionally fused with a portion of *PIR4* ORF. The

fusion had been obtained subcloning the amplified IL-1β coding sequence in the *BglII–SalI* sites of *PIR4* [9], with the loss of the carboxyterminal fragment of subunit II of Pir4 that contains three of the four highly conserved cysteine residues that are responsible for cell wall retention of Pir4 through disulphide bridges [8].

To this purpose, the recombinant strain obtained by transformation, indicated as *S. cerevisiae* CEN.PK113-5D [PIR4-IL1β], was tested for the expression and secretion of Pir4-IL1β fusion protein to the growth medium. For this, supernatants from shake-flask cultures of the recombinant strain were concentrated, and probed by immuno-blot analysis in Bio-Dot® (see below Analyses, IL-1β determination).

Fed-Batch Cultures

Fed-batch cultures were performed in a 2.0 L working volume of a stirred fermenter, Bioflo110 (New Brunswick Scientific). For all the strains examined, the fermenter initially contained 1 L of a medium prepared according to Verduyn et al. [12] with vitamins and trace elements. The medium was supplemented with 10 g L^{-1} of casamino acids (BD Bacto TM Casamino Acids, Becton–Dickinson & Co., Sparks, MD 21152 USA) and in the case of non-transformed strain 1.65 g L^{-1} of uracil according to Pronk [13], to fully cover strain requirements for the entire fermentation run.

The initial glucose concentration was 2 % w/v. The fermenter, was inoculated with an adequate aliquot of an exponential pre-culture in shake flasks prepared in the same conditions above described (except for uracil which was at a 15 mg L^{-1} concentration) to give an initial $O.D._{590}$ of 0.04. Fed-batch cultures were started by feeding the reactor with an exponentially increasing flow rate after 15 h batch phase, when glucose was exhausted, and before ethanol produced in batch phase was completely oxidized. The feeding solution contained glucose (50 % w/v), salts, trace elements, glutamic acid and vitamins according to Paciello et al. [14].

The time-dependent flow rate could be written as:

$$F_{(t)} = F_{(0)}e^{\alpha t}$$

where $F_{(t)}$ is the time-dependent flow rate (m^3 h^{-1}), $F_{(0)}$ is the initial flow rate and α is the constant of the exponentially increasing feeding rate (h^{-1}) which, in ideal conditions [10], is equal to the specific growth rate, μ.

The experimental values of the specific flow rate, were chosen considering that the shift from fully respiratory to respiro-fermentative metabolism occurs at a critical μ value (μ_{crit}) represented by the 60 % of μ_{max} [15]. In the case of CEN.PK113-5D strain, the μ_{crit} value was 0.31 h^{-1}, being μ_{max} 0.52 h^{-1} [6]. Therefore, the operative α values chosen in this work were 0.10, 0.16, 0.20 h^{-1}.

Oxygen was supplied to the reactor by air sparging. The dissolved oxygen tension (DOT) was kept at 30 % air saturation by the cascade system which acted, at first, on impeller speed, and when this latter reached its maximum value (1,000 rpm), on air enrichment with pure oxygen. The culture pH was maintained at 5.00 by automatic addition of 2 N KOH during batch phase, and 10 % v/v NH_4OH during fed-batch phase. The foam level in the fermenter was controlled by the automatic addition of a solution at 10 % v/v of antifoam B (Sigma Aldrich).

To test plasmid stability during growth, culture samples were withdrawn, properly diluted with 0.9 % NaCl and used to inoculate agar plates containing either non-selective (YPD medium: 2 % yeast extract, 1 % bactopeptone and 2 % glucose) or selective synthetic minimal medium SD (0.7 % yeast nitrogen base without amino acids, 2 % glucose, and uracil as required). Colony-forming units on the two different media, after 5 days of incubation at 30 °C, were evaluated and compared.

Biomass

Cell density was determined by optical density at 590 nm ($O.D._{590}$) and dry weight determination. The calibration curve relating $O.D._{590}$ values to the biomass density provided a correlation factor of 2.30 $O.D._{590}$ $g^{-1}_{d.w.}$ L^{-1}.

Specific death rate constant, k_d, was determined as a first order kinetic rate constant by plotting the ratio CFU mL^{-1}/$O.D._{590}$ vs. time, where CFU corresponded to the colony-forming units on YPD agar plates, originated by viable cells, and $O.D._{590}$ corresponded to the total amount of cells in the medium.

Catalase activity

Catalase activity was determined in the supernatants coming from cell extracts, prepared as follows: yeast cells, collected at different times of the fed-batch runs, were washed twice with 20 mM phosphate buffer, pH 7.0 and resuspended in 200 µL of the same buffer containing 1 mM EDTA and 0.1 mM PMSF. Cells were crushed with 0.4 mm diameter glass beads for 20–30 min (shaking for 1 min and placing the sample on ice for another 1 min, alternatively). Then, the cell homogenate was centrifuged (4,000 rpm, 15 min) and the supernatant was used for catalase assays. Catalase activity was measured by monitoring H_2O_2 decomposition at 240 nm at 25 °C. The supernatant, obtained as previously described, was quickly added to a solution containing 50 mM phosphate buffer and 13 mM H_2O_2 and the decrease in absorbance at 240 nm was measured after 1 min.

Analyses

IL-1β Determination

Samples were quickly withdrawn from fed-batch cultures, filtered on 0.45 μm GF/A filters (millipore, Bedford, MA, USA) and filtrates analyzed to determine interleukin-1β concentrations. Interleukin-1β was determined by immuno-blot analysis in Bio-Dot® Microfiltration Apparatus (Bio-Rad, Hercules, CA, USA) using the human IL-1β (EuroClone) as a standard. The nitrocellulose membranes were then treated with primary antibody (Rabbit polyclonal IgG IL-1β, Santa Cruz Biotechnology). IL-1β was quantified by dot blot analysis in ImageJ Software. All the samples were analyzed in triplicate and the values of standard deviation obtained were always under 5 %.

Glucose, ethanol, glycerol and acetate determination

Glucose, ethanol and glycerol in the growth medium were measured by high performance liquid chromatography [16]. Acetate concentration was determined using enzymatic assays (K-ACET kits from Megazyme).

ROS detection and viability determination

All measurements of fluorescence intensity were performed on a Cytomics FC 500 flow cytometer (Beckman Coulter) equipped with an argon laser (excitation wavelength 488 nm, laser power 20 mW). A total of 30,000 cells was measured for each sample. Data analysis was performed afterwards using WinMDI 2.8 software.

The presence of reactive oxygen species (ROS) was detected with dihydrorhodamine 123 (DHR) (Sigma Aldrich) as follows. Cell samples were taken during the run and diluted up to $O.D._{660} = 0.25$. Dilution was carried out with 3 mL of cell-free growing medium, collected at the same time and filtered through a 0.22 μm sterile filter. 7 μL of 123-DHR were added from a 1 mg mL^{-1} stock solution in ethanol and cells were incubated for 75 min at 30 °C. After three washes in PBS, cells were sonicated and fluorescence was measured at a single-cell level. The percentage of cells showing ROS accumulation was estimated by comparing the fluorescence distributions obtained with cells growing in exponential balanced phase on glucose (negative control) or exposed to H_2O_2 3 mM (positive control).

The percentage of dead cells in the population has been obtained after a propidium iodide (PI) staining. Briefly, 1×10^7 cells were collected, washed in PBS, resuspended in a volume of 40 μL, added with 5 μL of PI from a stock solution of 50 μg mL^{-1} and incubated for 20 min at room temperature. Cells were then washed twice in PBS and sonicated before analysis. Cells were scored as positive (i.e., dead) when their fluorescence fell within a gate established with a positive control obtained with the incubation of a sample in ethanol 70 % v/v for 15 min. Natural fluorescence of exponentially growing cells (negative control) completely fell below the gate.

Mathematical model

The mathematical model for the fed-batch reactor took into consideration only the fed-batch phase and was developed on the basis of the mass balance equations of three variables of interest, i.e., cell density (Eq. 1), residual glucose (Eq. 2), and ethanol (Eq. 3), concentrations [6]. The differential equations (listed below) with the corresponding initial conditions, were solved numerically by the Eulero's method [10]

$$\frac{dX}{dt} = -\frac{F}{V}X + \left[\mu_{Gi} + \left(\frac{(\mu_{max})_E \cdot E}{(k_S)_E + E}\right)(1-\beta) - k_d\right]X \qquad (1)$$

$$i = 1, 2$$

$$\frac{dG}{dt} = \frac{F}{V}(G_R - G) - \left[\frac{\mu_{Gi}}{\left((Y)_{X/G}\right)_i}\right]X \qquad i = 1, 2 \qquad (2)$$

$$\frac{dE}{dt} = -\frac{F}{V}E + \left[-\frac{\left(\frac{(\mu_{max})_E \cdot E}{(k_S)_E + E}\right)}{\left((Y)_{X/E}\right)}(1-\beta) + \mu_{G2} \cdot (Y)_{X/E}\right]X \qquad (3)$$

The following total mass balance on the culture volume was considered:

$$\frac{dV}{dt} = F \qquad (4)$$

The mathematical model assumed that yeast population was capable to utilize simultaneously the ethanol produced during batch phase and glucose fed to the reactor (Eq. 1). However, ethanol-assimilating enzymes are tightly regulated in *S. cerevisiae* at the level of enzyme synthesis and catabolite inactivation mediated by glucose [17]. Considering this, the model assumed that ethanol was consumed according to the Monod model corrected by a subtractive factor β, which permitted to take into account the inhibitory effect exerted by glucose on ethanol consumption (Eqs. 1, 3).

Cell death was also considered by introducing in the balance equation of biomass (Eq. 1) k_d, the specific death rate experimentally evaluated (see Sect. "Biomass").

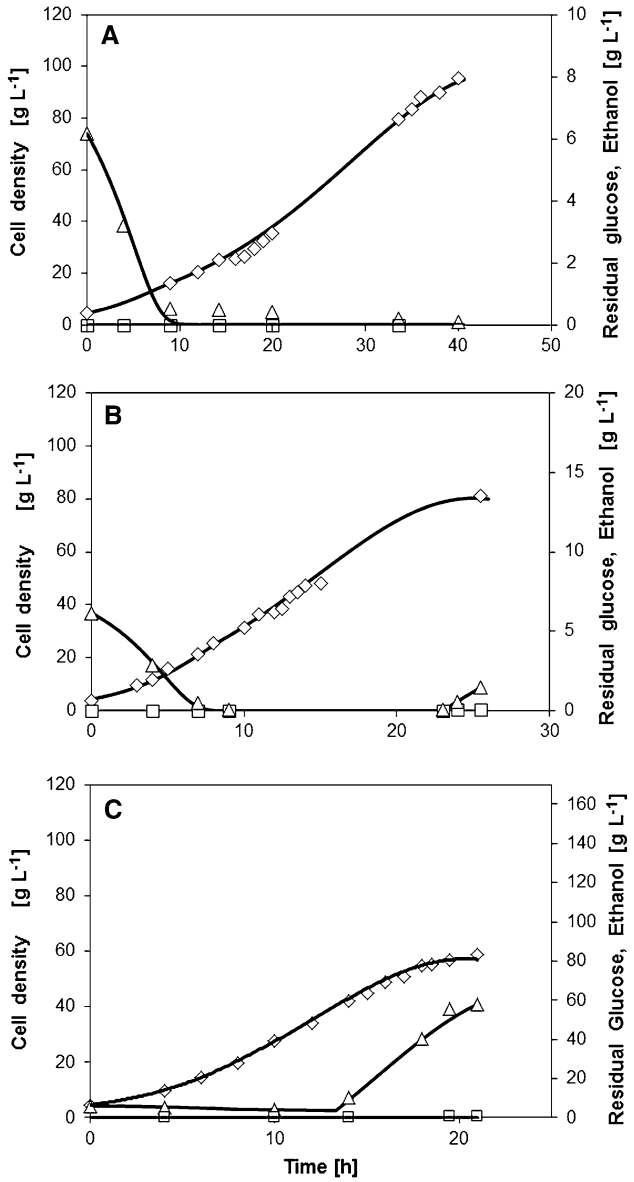

Fig. 1 Proliferation of non-transformed *S. cerevisiae* CEN.PK113-5D during fed-batch phase: experimental data and simulation curves (*continuous lines*) refer to cell density (*rhombus*), residual glucose (*square*), and ethanol (*triangle*) at three different specific flow rates: 0.10 h^{-1} (**a**) 0.16 h^{-1} (**b**) and 0.20 h^{-1} (**c**). The parameters used for simulations are reported in Table 2

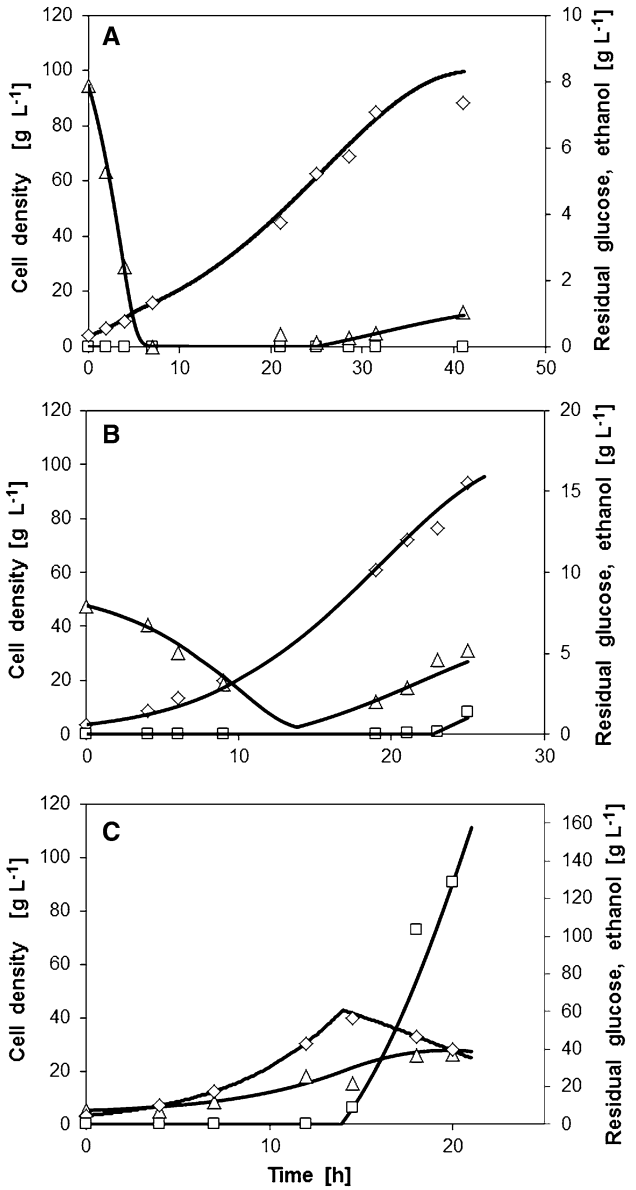

Fig. 2 Proliferation of recombinant *S. cerevisiae* CEN.PK113-5D [PIR4-IL-1β] during fed-batch phase: experimental data and simulation curves (*continuous lines*) refer to cell density (*rhombus*), residual glucose (*square*), and ethanol (*triangle*) at three different specific flow rates: 0.10 h^{-1} (**a**), 0.16 h^{-1} (**b**) and 0.20 h^{-1} (**c**). The parameters used for simulations are reported in Table 2

The metabolic quotient for glucose (Eq. 2) was expressed as the ratio $\frac{(\mu_G)_i}{((Y)_{X/G})_i}$, where the biomass yield value (observed yield) was inclusive of maintenance. Another modeling assumption was that ethanol could not be consumed and produced by cells at the same time. Ethanol specific production rate was given by $\mu_{G2}.(Y_{E/X})_P$, the product between specific growth rate on glucose and ethanol yield on biomass (Table 2).

Results

Fed-batch cultures of non-transformed and recombinant *S. cerevisiae* CEN.PK113-5D strains growing at different feeding rates: modeling and optimization

A series of three aerated fed-batch cultures was set up for both the non-transformed and the recombinant *S. cerevisiae* CEN.PK113-5D strain, supplying each culture with the

Table 1 Yield and volumetric productivity of biomass and product (IL-1β) for both the non-transformed and the recombinant *S. cerevisiae* CEN.PK 113-5D at different specific flow rates

Specific flow rate, α (h^{-1})	Non-transformed			Recombinant		
	0.10	0.16	0.20	0.10	0.16	0.20
Biomass yield on glucose ($g_{d.w.}$ g^{-1})	0.46	0.40	0.25	0.36	0.35	0.11
Biomass productivity ($g_{d.w.}$ L^{-1} h^{-1})	2.40	3.62	2.93	2.20	3.72	1.45
IL-1β yield on biomass (mg $g_{d.w.}^{-1}$)	–	–	–	0.08	0.08	0.08
IL-1β productivity (g L^{-1} h^{-1})	–	–	–	0.18	0.30	0.11

same amount of glucose (450 g). Glucose was fed to the fermenter at three different exponentially increasing feeding rates so the bioprocess length depended on the α value, the higher was the α value, the shorter was the run duration (Figs. 1, 2). In these conditions, the highest final cell density for the non-transformed strain was achieved when the reactor was fed at the lowest α value 0.10 h^{-1} (Fig. 1a). By increasing α up to 0.16 (Fig. 1b) and 0.20 h^{-1} (Fig. 1c), the final cell density decreased, achieving at α 0.2 h^{-1}, only 60 % of the cell density obtained at α 0.1 h^{-1}.

Table 1 shows the values of biomass yield on glucose and the volumetric biomass productivity. The average biomass yield on glucose shifted from 0.46 (a typical value for respiratory metabolism) obtained at 0.10 h^{-1} α value, to 0.25 when α was enhanced up to 0.2 h^{-1}, highlighting a shift towards a fermentative metabolism. This metabolic shift was also confirmed by ethanol accumulation (Fig. 1c). Biomass volumetric productivity reached a maximum at α 0.16 h^{-1}.

When *S. cerevisiae* CEN.PK113-5D was transformed for IL-1β expression and cultured in the same conditions as the non-transformed strain, the cell density profiles obtained carrying out fed-batch runs at 0.10 and 0.16 h^{-1} α values (Fig. 2a, b, respectively), exhibited a rather similar trend if compared to the non-transformed strains. In contrast, at α 0.20 h^{-1} α value, the final cell density was only 40 g L^{-1} after 14 h of feeding (Fig. 2c), then it sharply diminished.

In the case of the recombinant strain as well, the values of biomass yield on glucose (Table 1) decreased with increasing value of α, and were lower than those obtained with the non-transformed strain. Product yield on biomass, experimentally determined, was constant as expected for a growth-associated product and amounted to 0.08 mg $g_{d.w.}^{-1}$ (Table 1) independently of the specific feeding rate employed. Maximum productivity of IL-1β was obtained at the α value of 0.16 h^{-1} (Table 1). No plasmid loss from *S. cerevisiae* [PIR4-IL1β] cells was observed after 72 h incubation, since the number of colony-forming units appearing on either selective or non-selective agar plates were the same.

Except for the recombinant strain cultured at 0.20 h^{-1} α value (Fig. 2c), in all other cases residual glucose was undetectable for almost all the duration of the run (Figs. 1a, b, 2a, b). Therefore, glucose supplied to the fermenter was entirely consumed, so that *S. cerevisiae* CEN.PK 113-5D should be able to grow on glucose at a specific growth rate (μ_G) equal to the α value imposed. Actually, μ_G values (Table 2) maintained close to the α value only in the early phase of feeding μ_{G1}, when the yeast cells consumed simultaneously ethanol (produced during the batch phase) and glucose until t_{EC}, the time point at which glucose inhibition blocks ethanol consumption. After t_{EC}, μ_G decreased exponentially with time (μ_{G2}). This behavior was confirmed by the good agreement between simulation curves and experimental data related to process variables considered (cell density, residual glucose and ethanol) both for the non-transformed strain (Fig. 1) and the recombinant strain (Fig. 2). The values of β (Table 2), representing the level of glucose inhibition on ethanol consumption, directly depended on α values.

To describe the behavior of yeast cells when ethanol consumption was totally inhibited by glucose, the kinetic parameters were changed over time (Table 2), taking also into account the progressive diversion of metabolism towards fermentation, as highlighted by the onset of ethanol in the late feeding phase.

The values of biomass yield on glucose $[(Y)_{X/G}]_1$ and $[(Y)_{X/G}]_2$ (Table 2), before and after the time t_{EC}, respectively, confirmed that the initial respiratory metabolism was fated to progressively shift towards a fermentative one, this latter in agreement with the ethanol production observed during the runs (Figs. 1, 2). In the case of the non-transformed CEN.PK113-5D strain, ethanol appeared only at the end of the run carried out at 0.16 h^{-1}α value (Fig. 1b), and it was produced in a significant amount during the run carried out at α 0.20 h^{-1} (Fig. 1c), even if with different values of ethanol (as product) yield on biomass $[(Y)_{E/X}]_P$, (Table 2).

On the contrary, for the recombinant strain, ethanol production was already observable at 0.10 h^{-1} α value (Fig. 2a). Apparently, the transformation of CEN.PK113-5D with a multicopy plasmid carrying the heterologous information, determined a metabolic burden related to an earlier metabolic shift from respiration to fermentation well described by new kinetic parameters (Table 2). The lowest performance was achieved with the recombinant strain cultured at 0.20 h^{-1} α value, which ceased to grow after 14 h of feeding (Fig. 2c).

Considering these results and in the perspective to optimize the production of IL-1β by reducing the process

Table 2 Parameters of the mathematical model for the non-transformed and the recombinant *S. cerevisiae* CEN.PK113-5D

Specific flow rate, α (h^{-1})	Non-transformed			Recombinant		
	0.10	0.16	0.20	0.10	0.16	0.20
X_o(g L^{-1})	4.62	4.62	4.62	3.56	3.63	3.24
G_0(g L^{-1})	0	0	0	0	0	0
E_0(g L^{-1})	6.17	6.24	6.05	7.90	7.95	7.41
$(\mu_G)_1$(h^{-1})	0.09	0.17	0.20	0.10	0.18	0.215
$(\mu_G)_2$(h^{-1})	0.09exp(−0,009(t−8.2))	0.135exp(−0,031(t−8.2))	0.19exp(−0.037(t−7))	0.10exp(−0.019(t−6.7))	0.16exp(−0.024(t−10))	0
t_{EC}(h)	8.2	8.2	7	6.7	10	14
t_{EP}(h)	–	23	13.3	28.5	7.3	0
k_d(h^{-1})	0	0	0.012	0	0	0.016
$(\mu_{max})_E$(h^{-1})	0.10	0.10	0.10	0.20	0.20	–
k_s(g L^{-1})	1.8	1.8	1.8	1.8	1.8	1.8
β	0.028	0.06	0.84	0.004	0.89	1
$\left[(Y)_{X/E}\right]_S$(g g^{-1})	0.68	0.68	0.68	0.68	0.68	0.68
$\left[(Y)_{X/G}\right]_1$(g g^{-1})	0.44/0.66	0.53/0.84	0.49/0.50	0.50/0.70	0.57/0.69	0.50/0.52
$\left[(Y)_{X/G}\right]_2$(g g^{-1})	0.22/0.66	0.14/0.67	0.11/0.46	0.20/0.70	0.14/0.92	–
$\left[(Y)_{E/X}\right]_P$(g g^{-1})	–	0.10/0.11	1.26/1.68	0.013/0.017	0.022/0.052	0.50/0.506

t_{EC} time at which the ethanol consumption stops; t_{EP} time at which the ethanol production begins

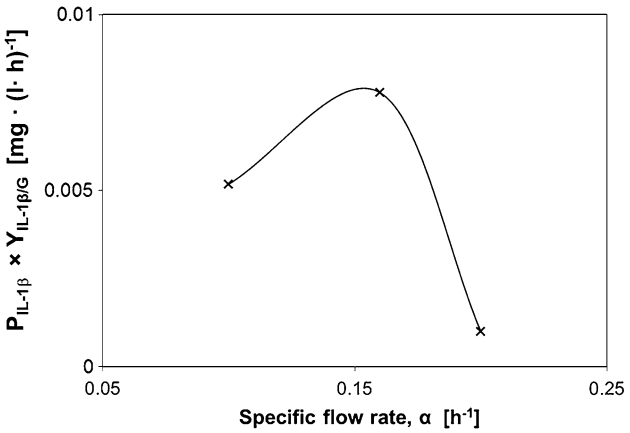

Fig. 3 Bioprocess optimization: product between IL-1β volumetric productivity and IL-1β yield on glucose plotted against the specific flow rate

Table 3 Stress indicators and cell viability for the non-transformed and the recombinant *S. cerevisiae* CEN.PK 113-5D

Specific flow rate (h^{-1})	Non-transformed			Recombinant		
	0.10	0.16	0.20	0.10	0.16	0.20
Glycerol[a] (g L^{-1})	<0.01	<0.01	<0.01	0.26	0.52	4.03
Acetate[b] (g L^{-1})	ND	<0.015	0.160	<0.015	0.025	0.351
ROS[c] (%)	9.9	14.2	17.3	11.2	16.4	21.0
PI[d] \(%)	ND	6.5	8.8	6.2	7.44	9.6

ND not detectable

[a] Maximum glycerol concentration

[b] Acetate concentration at the onset of ethanol production

[c] Maximum percent of population showing ROS accumulation

[d] Percent of population showing PI accumulation at the onset of ethanol production

time and the amount of glucose consumed, the product between IL-1β volumetric productivity and IL-1β yield on glucose was plotted against the specific feeding rate (Fig. 3). The interpolation of the experimental data indicated that the bioprocess optimization was achievable at an α value close to 0.16 h^{-1}.

Fed-batch cultures of non-transformed and recombinant *S. cerevisiae* CEN.PK113-5D strains growing at different feeding rates: physiological aspects

As shown in the previous section, during fed-batch culture the onset of ethanol production was observed both for the non-transformed and the recombinant strain, notwithstanding the fed-batch runs were performed at μ values lower than the critical one [11]. Further, this behavior appeared to be related to the feeding rate and, at the same feeding rate, it was more significant in the case of the recombinant strain.

In an attempt to gain a deeper insight into the unexpected shift of the yeast metabolism towards fermentation, some other metabolic and physiological indicators have been considered.

Determination of cell viability by propidium iodide (PI) staining (Table 3) demonstrated that almost the totality of the cells, at the onset of ethanol production, resulted viable. A small increase of the percent of population showing PI accumulation was observed only when cultures were performed at 0.20 h^{-1} α value, in agreement with the very low k_d values measured at the same α value (Table 2).

Therefore, we verified the possibility that the decrease in biomass yield and ethanol appearance were due to the high cell density and to a local insufficient oxygen supply that triggered the onset of a fermentative metabolism despite the control imposed on DOT. Since glycerol is a redox sink when the mitochondrial re-oxidation of cytoplasmic NADH is impaired [18], it can be considered as an indicator of a metabolic shift towards fermentation. Actually, in our samples (Table 3), glycerol accumulation was observed only in the case of the recombinant strain, with the highest concentration found in the case of yeast cells growing at a feeding rate of 0.20 h^{-1}. Acetate is another typical fermentative metabolite that could also induce an abnormal ATP requirement due to its uncoupling effect [19]. Table 3 also reports acetate concentrations in samples collected just after ethanol appearance. At any α value considered, acetate concentration resulted rather low, with the highest value (0.351 mg L^{-1}) achieved by the recombinant strain grown at 0.20 h^{-1} α value.

Finally, we explored the possibility that the decrease in biomass yield was related to the occurrence an oxidative stress, so that we measured the accumulation of reactive oxygen species (ROS), as well as the induction of the detoxifying enzyme catalase. As regards ROS, no relevant accumulation was observed in every operative condition examined (Table 3), since most of the population displayed fluorescence levels comparable to a control population growing on glucose in exponential balanced phase (data not shown).

As regards catalase, the specific enzyme activity of the non-transformed strain cultured at 0.10 h^{-1} (Fig. 4a) achieved its maximum after about 10–12 h of feeding, then the activity diminished but retained a significantly high value until the end of feeding. Increasing the feed rate up to 0.16 h^{-1}, catalase activity retained a similar pattern, and dramatically dropped when the feed rate was raised up to 0.20 h^{-1}. Contrarily, in the case of the recombinant strain (Fig. 4b), catalase activity exhibited a lower value along

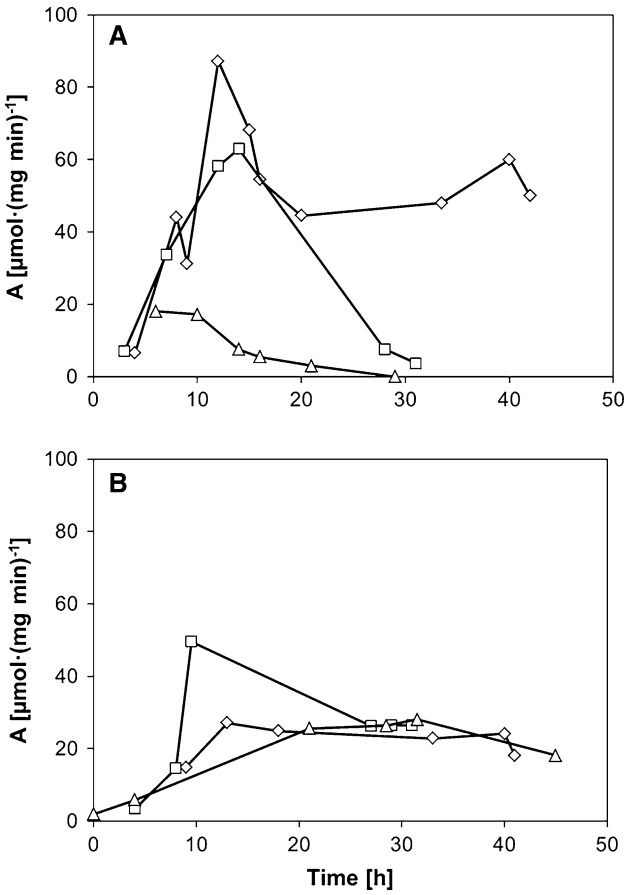

Fig. 4 Catalase activity of *S. cerevisiae* CEN.PK113-5D growing in aerated fed-batch reactor: time-course of specific catalase activity of non-transformed (**a**) and recombinant (**b**) strain at three different specific flow rates: 0.10 h^{-1} (*rhombus*) 0.16 h^{-1} (*square*) and 0.20 h^{-1} (*triangle*)

the entire fermentation run for all the α values examined, except for the point after 12 h of feeding at 0.1^{-1} α value.

Discussion

Setting up of high cell densities cultures in the case of growth-associated products is a pre-requisite for high productivity, though significant values of microbial cell density per volume unit (80–100 $g_{d.w.}$ L^{-1} in the case of yeast) are not always easily achieved [1].

In aerobic cultures of *S. cerevisiae,* alcoholic fermentation and respiration occur simultaneously when the sugar concentration exceed a critical value [20, 21]. Alcoholic fermentation has to be avoided during heterologous protein production because it negatively affects biomass yield, ATP yield from fermentation being much lower than from respiratory sugar dissimilation [22]. Therefore, in fed-batch reactor, growth rate must be controlled by supplying the bioreactor at a proper feed rate [5].

In the present work, aiming both at optimizing the volumetric productivity and understanding to what extent the environmental conditions could affect the yeast performance, the strain CEN.PK113-5D, belonging to the CEN.PK113 series widely used for metabolic engineering and systems biology research in industry and academia [23], either as such or transformed, was allowed to grow at constant specific growth rates below the critical value by replenishing the fermenter with three different exponentially increasing feeding profiles. The rationale behind this optimization study, resided on the possibility of reducing the working time by acting on the operative conditions, since other factors of implementation such as selection of suitable host with a high specific growth rate [6], efficient expression system [9], and proper medium composition [14] had already been investigated.

Our results have shown that a good compromise between volumetric productivity and biomass yield was reached with the recombinant strain fed at an α value (0.16 h^{-1}).

Beyond the predictions regarding the possibility of controlling yeast metabolism through a suitable feeding, the results obtained in this work have shown that the metabolic shift from respiration to fermentation can occur even below the critical threshold (0.3 h^{-1}).

In this respect, the behavior of the recombinant strain resulted more pronounced, with ethanol being produced at any α value, causing a relevant decrease in cellular yield. The different behavior observed between the non-transformed and the recombinant strain suggests that IL-1β production can alter cell physiology, even if produced in little amounts (0.08 mg g^{-1} cells d.w., Table 1). It has been widely reported that heterologous protein production may impose a metabolic burden on the host cells, with the diversion of anabolic precursors and energy from normal growth towards maintenance. The effect of metabolic burden on several cell parameters, such as specific growth rate, biomass yield, respiratory capacity and energy requirements have been described [24, 25], being a decrease in growth rate the most commonly observed phenomenon. Moreover, the deleterious effects of metabolic burden on cell physiology have been shown to depend on the kind of protein expressed, and not simply proportional to the amount of the heterologous product itself [25]. Therefore, it is likely that an increased demand of glycolytic intermediates or ATP imposed by IL-1β synthesis may commit the recombinant strain towards fermentative metabolism, i.e. the metabolism usually triggered by stressful conditions [26].

Aiming to explain the metabolic shift towards fermentation, some possible hypotheses have been formulated. Ethanol fermentation could be a consequence of an insufficient oxygen supply related to the high biomass

concentration, despite the control imposed on DOT. However, looking at the accumulation of glycerol (Table 3), a metabolite that is typically produced during the fermentative metabolism, when mitochondrial activity is insufficient to maintain a correct redox balance [18], the hypothesis of low oxygenation had to be discarded since it was found to be unrelated to ethanol formation. In fact, glycerol was present only in samples from the recombinant strain (Table 3), while aeration conditions were the same for both the strains (with a DOT value kept at 30 % air saturation over the runs) and glycerol accumulation was not significant in the case of the non-transformed strain, which produced ethanol as well (Fig. 1c).

Alternatively, ethanol formation could be the effect of the presence of relevant amounts of weak organic acids, such as acetic acid. Acetic acid is a potent inhibitor of yeast growth and survival [27, 28], and its uncoupling effect requires relevant amounts of ATP, increasing the glycolytic flux with ethanol accumulation and decrease in biomass yields [29]. However, the involvement of acetic acid in the observed phenomenon is unlikely, since even the highest amount of acetic acid detected (Table 3) was too low to be considered responsible for an uncoupling phenomenon leading to ethanol production [19], considering also that at pH 5 only 60 % of the metabolite is in its non-dissociated form.

Ethanol formation occurred more or less concomitantly with the progressive reduction of the proliferative capacity of the yeast population, as shown by the exponentially decreasing of the specific growth rates on glucose (μ_G) during the runs (Table 2). This phenomenon could be attributed to a possible oxidative stress exerted on yeast cells during cultivation, so that some stress indicators such as acetate concentrations, ROS accumulation, and cell viability were evaluated. Putting all the data together, it appeared that, during the runs, the majority of cells of both strains were healthy and viable, since acetate concentrations in the growth medium and ROS formation were negligible.

As regards catalase, this enzyme deserves a separate mention. It is well known that its detoxifying action occurs through the removal of hydrogen peroxide [30], a deleterious substance produced during respiration [31]. Considering this role, high catalase activity levels have to be related to the occurrence of a fully respiratory metabolism. Not surprisingly, the highest levels of catalase activity were detected in the case of the non-transformed strain which kept a respiratory metabolism all over the run when it was fed at the lowest α value. On the other hand, the recombinant strain, which showed a more precocious and marked shift towards fermentation, never exhibited high levels of catalase activity during the runs.

Modeling of the fed-batch reactor was a useful tool to describe the inhibition exerted by glucose on ethanol consumption and to support the experimental evidence that the metabolic shift depended on the rate of glucose supply, and took place earlier the higher was the feed rate. This behavior was more pronounced in the case of the recombinant strain.

Undoubtedly, the model proposed reveals some limits due to the fact that it is an unstructured model that works well in the early phase of the fed-batch run, where the parameters can be assumed constant with time. To describe the bioprocess in the following hours, it is necessary an adjustment of these parameters during the time-course, due to the occurrence of metabolic fluctuations of yeast cells in that peculiar environment of growth.

In conclusion, our results have shown that in high cell density cultures yeast growth unavoidably declines, leading to undesired ethanol accumulation. The phenomenon was more evident if cell metabolism had to sustain the production of a heterologous product, with the consequent metabolic burden derived from the presence of a particular construct. Growth of CEN.PK113-5D strain did not seem to be significantly affected by neither inefficient oxygenation of the culture nor oxidative stress phenomena. However, the decline of the proliferative capacity of the yeast cells after a relatively short period of feeding, and the transition to a fermentative metabolism remain to be clarified. Clarifying these still unknown aspects of yeast behavior represents a challenge that can be best answered using high cell density cultures in fed-batch reactors.

Acknowledgments This research was supported by the University of Salerno funds (FARB, 2011) to Palma Parascandola in the framework of the research project “Ottimizzazione e modellazione di sistemi HCDC (high cell-density cultivation) per la produzione di masse microbiche da lievito: parametri biologici e condizioni di processo”.

References

1. Riesenberg D, Guthke R (1999) High-cell-density cultivation of microorganisms. Appl Microbiol Biotechnol 51(4):422–430
2. Shojaosadati SA, Varedi SMK, Babaei Pour V, Farnoud AM (2008) Recent advances in high cell density cultivation for production of recombinant protein. Iran J Biotechnol 6:63–84
3. Martinez JL, Liu L, Petranovic D, Nielsen J (2012) Pharmaceutical protein production by yeast: towards production of human blood proteins by microbial fermentation. Curr Opin Biotechnol 23:965–971
4. Mattanovich D, Branduardi P, Dato L, Gasser B, Sauer M, Porro D (2012) Recombinant protein production in yeasts. Methods Mol Biol 824:329–358
5. Beudeker RF, van Dam HW, van der Plaat JB, Vellega K (1990) Developments in bakers’ yeast production. In: Verachtert H, De Mot R (eds) Yeast biotechnology and biocatalysis. Marcel Dekker, New York
6. Landi C, Paciello L, de Alteriis E, Brambilla L, Parascandola P (2011) Effect of auxotrophies on yeast performance in aerated fed-batch reactor. Biochem Biophys Res Comm 414:604–611

7. Andrés I, Gallardo O, Parascandola P, Pastor J, Zueco J (2005) Use of the cell wall protein Pir4 as a fusion partner for the expression of *Bacillus* sp.BP-7 xylanase A in *Saccharomyces cerevisiae*. Biotechnol Bioeng 89:690–697
8. Moukadiri I, Jafar L, Zueco J (1999) Identification of two mannoproteins released from cell walls of *Saccharomyces cerevisiae* mnn1 and mnn9 double mutant by reducing agents. J Bacteriol 181:4741–4745
9. Paciello L, Andrès I, Zueco J, Bianchi MM, de Alteriis E, Parascandola P (2010) Expression of human interleukin-1β in *Saccharomyces cerevisiae* using PIR4 as fusion partner and production in aerated fed-batch reactor. Ann Microbiol 60:719–728
10. Enfors SO, Häggström L (1998) Bioprocess technology: fundamentals and applications. Royal Institute of Technology, Stockholm
11. Porro D, Brambilla L, Alberghina L (2003) Glucose metabolism and cell size in continuous cultures of *Saccharomyces cerevisiae*. FEMS Microbiol Lett 229:165–171
12. Verduyn C, Postma E, Scheffers WA, van Dijken JP (1992) Effect of benzoic acid on metabolic fluxes in yeasts: a continuous study on the regulation of respiration and alcoholic fermentation. Yeast 8:501–517
13. Pronk JT (2002) Auxotrophic yeast strains in fundamental and applied research. Appl Environ Microbiol 68:2095–2100
14. Paciello L, de Alteriis E, Mazzoni C, Palermo V, Zueco J, Parascandola P (2009) Performance of the auxotrophic *Saccharomyces cerevisiae* BY4741 as host for human interleukin-1β production in an aerated fed-batch reactor. Microb Cell Fact 8:70–82
15. Enfors SO (2001) Baker's yeast. In: Ratledge C, Kristiansen B (eds) Basic Biotechnology. Cambridge University Press, Cambridge
16. Camattari A, Bianchi MM, Branduardi P, Porro D, Brambilla L (2007) Induction by hypoxia of heterologous-protein production with the KlPDC1 promoter in yeasts. Appl Env Microbiol 73:922–929
17. Willis C (1990) Regulation of sugar and ethanol metabolism in *Saccharomyces cerevisiae*. Crit Rev Biochem Mol Biol 25:245–280
18. Valadi A, Granath K, Gustafsson L, Adler L (2004) Distinct intracellular localization of Gpd1p and Gpd2p, the two yeast isoforms of NAD+-dependent glycerol-3-phosphate dehydrogenase, explains their different contributions to redox-driven glycerol production. J Biol Chem 279(38):39677–39685
19. Verduyn C, Postma E, Scheffers WA, van Dijken JP (1990) Energetics of *Saccharomyces cerevisiae* in anaerobic glucose-limited chemostat cultures. J Gen Microbiol 136:405–412
20. De Deken RH (1966) The crabtree effect: a regulatory system in yeast. J Gen Microbiol 44:149–156
21. Petrik M, Käppeli O, Fiechter A (1983) An expanded concept for glucose effect in the yeast *Saccharomyces uvarum:* involvement of short- and long-term regulation. J Gen Microbiol 129:43–49
22. van Hoek P, Flikweert MT, van Der Aart QJM, De Steensma HY, van Dijken JP, Pronk JT (1998) Effects of pyruvate decarboxylase overproduction on flux distribution at the pyruvate branch point in *Saccharomyces cerevisiae*. Appl Env Microbiol 64:2133–2140
23. Nijkamp JF, van den Broek M, Datema E, de Kok S, Bosman L, Luttik MA, Daran-Lapujade P, Vongsangnak W, Nielsen J, Heijne WHM, Klaassen P, Paddon CJ, Platt D, Kötter P, van Ham RC, Reinders MJT, Pronk JT, de Ridder D, Daran JM (2012) De novo sequencing, assembly and analysis of the genome of the laboratory strain *Saccharomyces cerevisiae* CEN.PK113-7D, a model for modern industrial biotechnology. Microb Cell Fact 11:36
24. Glick BR (1995) Metabolic load and heterologous gene expression. Biotechnol Adv 13:247–261
25. Gorgens JF, van Zyl WH, Knoetze JH, Hahn-Hagerdal B (2001) The metabolic burden of the PGK1 and ADH2 promoter systems for heterologous xylanase production by *Saccharomyces cerevisiae* in defined medium. Biotechnol Bioeng 73:238–245
26. Molenaar D, van Berlo R, de Ridder D, Teusink B (2009) Shifts in growth strategies reflect tradeoffs in cellular economics. Mol Syst Biol 5:323–332
27. Semchyshyn HM, Abrat OB, Miedzobrodzki J, Inoue Y, Lushchak VIì (2011) Acetate but not propionate induces oxidative stress in bakers' yeast *Saccharomyces cerevisiae*. Redox Rep 16:15–23
28. Casatta N, Porro A, Orlandi I, Brambilla L, Vai M (2012) Lack of Sir2 increases acetate consumption and decreases extracellular pro-aging factors. Biochim Biophys Acta 1833:593–601
29. Postma E, Verduyn C, Scheffers WA, van Dijken JP (1989) Enzymic analysis of the Crabtree effect in glucose-limited chemostat cultures of *Saccharomyces cerevisiae*. Appl Env Microbiol 55:468–477
30. Chance B, Oshino N (1971) Kinetics and mechanisms of catalase in peroxisomes of the mitochondrial fraction. Biochem J 122:225–233
31. Petrova VY, Rasheva TV, Kujumdzieva AV (2002) Catalase enzyme in mitochondria of *Saccharomyces cerevisiae*. Electron J Biotechnol 5:29–41